

Design for CCAT, a 25 m diameter telescope operating from 200 GHz to 1.5 THz

David Woody¹, Steve Padin², Dave Redding³, John Lou⁴ and Andy Kissil⁵

¹Owens Valley Radio Observatory, Caltech, P.O. Box 968, Big Pine, CA 93513 USA, dwoody@caltech.edu

²Caltech, 1200 E. California Blvd., Pasadena, CA 91125 USA, sp@astro.caltech.edu

³JPL, 4800 Oak Grove Drive, Pasadena, CA 91109 USA, David.C.Redding@jpl.nasa.gov

⁴JPL, john.z.lou@jpl.nasa.gov

⁵JPL, Kissil, andrew.kissil@jpl.nasa.gov

Abstract

CCAT will be a 25 m diameter Ritchey-Chretien telescope operating in the 0.2–1.5 mm wavelength range. It will be located at an altitude of 5600 m on Cerro Chajnantor in northern Chile, near the ALMA site. CCAT will have an f/0.4 primary, with an active surface to compensate gravitational and thermal deformations. The primary will be supported by a carbon fiber reinforced plastic (CFRP) space frame truss on an elevation over azimuth mount made of steel. Cameras and spectrometers with up to 1 deg field of view (FoV) will be located at the two f/6 Nasmyth foci. CCAT will be inside an enclosure to reduce wavefront and pointing errors due to wind forces and thermal deformation due to solar illumination. The key performance challenges for CCAT are a half wavefront error (HWFE) <10 μm rms and pointing error <0.2".

1. Introduction

CCAT will be a large single aperture telescope optimized for wide-field mapping of the submillimeter sky and observations in the highest frequency submillimeter atmospheric windows accessible from the ground. The telescope will be equipped with very wideband spectrometers that instantaneously cover a full atmospheric window and wide field cameras with more than 10^5 pixels. The site on Cerro Chajnantor at 5600 m has low atmospheric opacity in the submillimeter atmospheric windows and even the 1.2 and 1.5 THz windows are usable from this site. A small beam size is needed to reduce the confusion noise and give accurate positions for high-resolution follow-up observations. At 25 m diameter and 350 μm wavelength, CCAT will have a 3.5" beam width, which is significantly smaller than any of the existing single aperture ground or space based telescopes in this frequency range.

The critical telescope specifications for achieving the performance goals for CCAT are a HWFE <10 μm rms and pointing better than 0.2", beyond the current state-of-the-art for large radio telescopes. The following sections describe the design solutions developed to meet these requirements at an affordable cost. Section 2 describes the telescope concept including the mount, truss and reflector segments. Section 3 describes the closed loop control of the surface and the inexpensive optical edge sensors used to measure the segment to segment displacements.

2. Telescope Configuration

Figure 1 show the major components for the CCAT telescope. It is an f/0.4 Ritchey-Chretien telescope with two f/6 Nasmyth foci accessed by rotating the tertiary. The optical path at the tertiary and through the elevation axle is 3 m diameter to accommodate the large 1 deg FoV and associated instruments [1]. The mount is a standard elevation over azimuth steel structure. Low friction hydrostatic bearings and magnetic direct drives are used for the azimuth and elevation axes to meet the very demanding pointing requirements.

CCAT will be protected from the weather by an enclosure which opens for observations. When open, the enclosure will also shield the telescope from the wind and provide a sun shade while the sun is below ~30 deg elevation. The f/0.4 design results in a very compact telescope with a 30 m diameter swept volume and a correspondingly modest sized enclosure.

A CFRP truss is used to support the reflector segments. CFRP with its high strength to weight ratio and low coefficient of thermal expansion (CTE) offers a large advantage over steel for large submillimeter telescopes but it is important to employ a method for attaching the CFRP truss to the steel tipping structure that doesn't compromise the truss stiffness and low thermal distortion. A couple of different interface methods based on thermal homology were

explored for CCAT which allow the steel structure to expand or shrink relative to the CRFP truss with minimal distortion of the reflector surface [2]. The concept shown in fig. 1 uses a ring of six azimuthal blade flexures between the truss and the steel tipping structure plus the addition of a central steel pillar connected to the truss with six CFRP radial struts. This configuration is very stiff, yielding a lowest resonant frequency for the full primary, secondary and tipping structure of ~ 8 Hz. The thermal distortion for a 20 C temperature changes is also small, $< 4 \mu\text{m}$ HWFE.

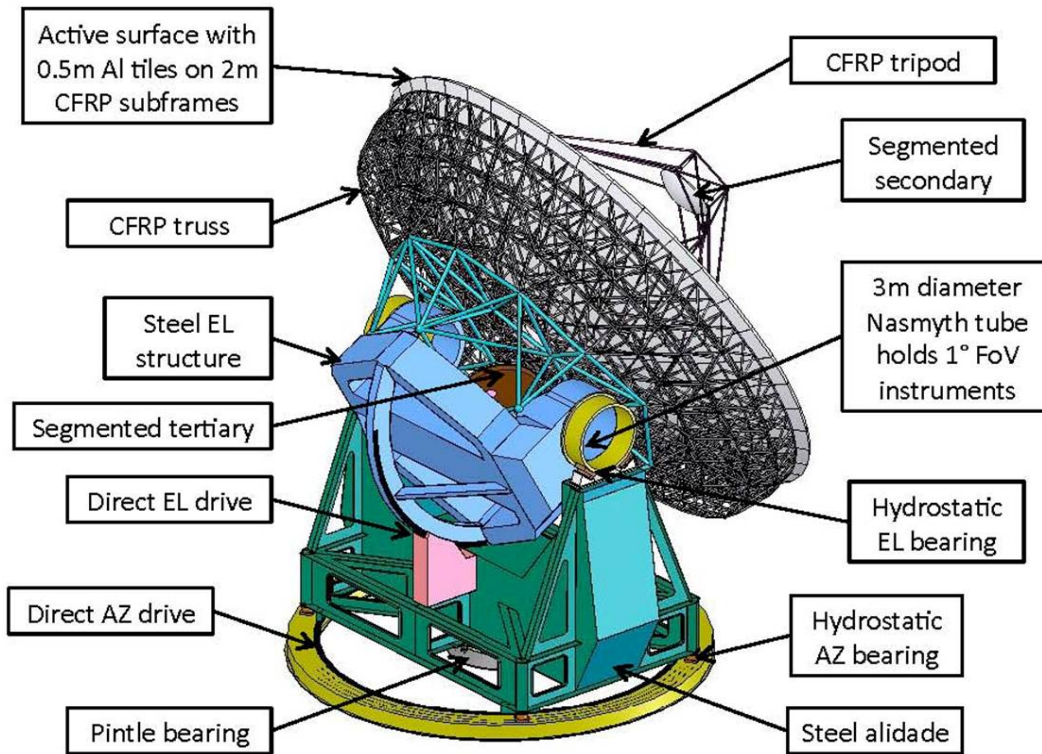


Fig. 1. Drawing of the major components for CCAT.

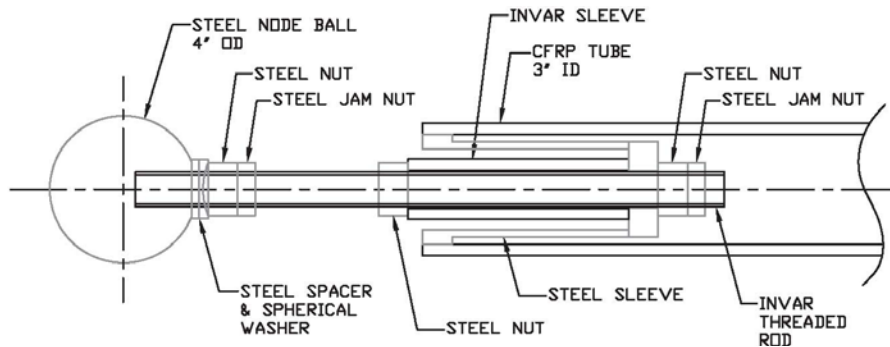


Fig. 2. Concept for truss strut which can be tailored to match the design CTE of 0.2 ppm/C for widely varying strut lengths and diameters.

The thermal performance of the truss is driven by both the few degree temperature gradients within the structure and the large +20 to -20 C operating temperature for the telescope. Meeting the surface error specification under these conditions requires that the average effective CTE be $< \sim 0.2$ ppm/C with a variation from strut to struts $< \sim 0.1$ ppm/C. The CFRP tubes used in the struts is essentially all uni-directional carbon fibers and will have a fairly uniform CTE of -0.5 ppm/C which in combination with steel and Invar end fittings and nodes produce the desired effective CTE. The end fitting design shown in fig. 2 can be tailored for each strut to achieve the 0.2 ppm/C CTE for all of the struts which range in length from 0.9 to 6.4 m and have diameters from 100 to 200 mm. The key concept is to use a reentrant steel end fitting which has the effect of reversing the sign the CTE for the steel, i.e. when the temperature increases the expansion of this component causes the length of the strut to decrease.

The primary reflector consists of 162 keystone shaped segments arranged in six circular rings. Each segment is mounted on three computer controlled actuators to correct for gravity and thermally induced distortions of the truss. The segments are ~2 m x 2 m and fabricating segments which meet the required surface error <math><5 \mu\text{m rms}</math> under all operating conditions is a challenge. The CCAT segments will consist of 4 to 16 reflector tiles mounted on a stiff and stable CFRP subframes [3]. The CFRP subframes will be insulated on all sides to further reduce the thermal distortions. Because of the relatively small size of the tiles several different materials and fabrication techniques can be utilized, including machined aluminum tiles.

3. Surface Figure Maintenance System

CCAT will have an active surface to maintain the primary figure. The gravity distortions can be corrected using a lookup table with actuator position as a function of elevation angle. This table can be generated from finite element analysis (FEA) of the structure plus detailed wave front measurements at a few elevations. Even with a high quality CFRP truss it is anticipated that the thermal distortions will degrade the surface for observations at the shortest wavelengths. There are no real time wavefront measurement techniques that work at submillimeter wavelengths, so the control procedures applicable to optical telescopes that utilize edge sensors plus wavefront measurement [4] are not applicable to CCAT.

A surface control system has been developed that reconstructs the wavefront from the perturbations of the segment positions and uses this information to determine the optimal motions of the three actuators supporting each segment [5]. The segment perturbations will be measured relative to the neighboring segments using a new type of edge sensor. The simulation of the control system for the gravity and thermal distortions indicates that the control is improved significantly when all six degrees of freedom (6DoF), not just the piston and dihedral angle between the segments, are measured at each boundary between segments. The control system uses a Kalman filter approach to account for expected or known distortions in the truss and in the individual segments as well as to optimally weight the sensor readings based on their noise. The simulations indicate that the expected gravity and thermal distortions can be corrected with an accuracy of <math><2 \mu\text{m rms}</math> HWFE wavefront error [6]. Figure 3 shows the perturbed wavefront due to gravity distortion at 45 deg elevation and the corrected wavefront after adjusting the segment actuators.

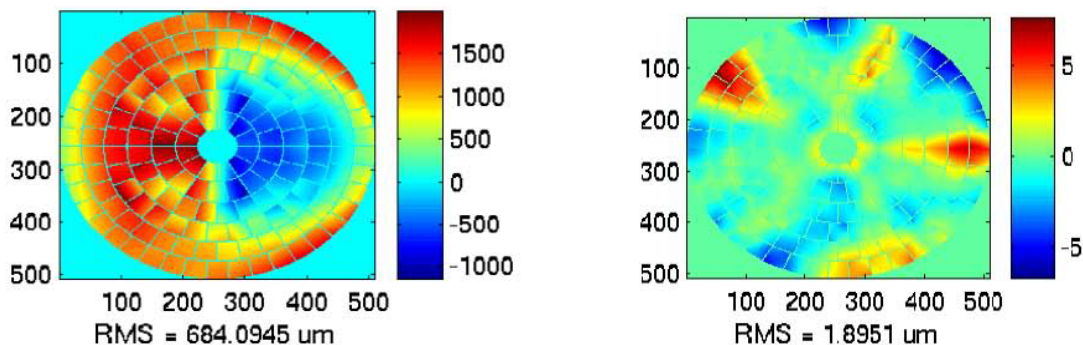


Fig. 3. The perturbed (left) and corrected (right) wavefront in μm for 1 G applied at 45 deg. The X and Y plot axes are in pixels for the ray tracing used to determine wavefront. The control simulations include $0.5 \mu\text{m}$ sensor measurement noise.

A critical part of this control system is the edge sensors. An inexpensive edge sensor has been developed for CCAT that measures all 6DoF motion between segments with an accuracy of <math><0.1 \mu\text{m}</math> for the three displacements and <math><1 \mu\text{rad}</math> for the three angles. The sensor system is based upon a novel imaging displacement sensor (IDS). The IDS uses a simple LED and pinhole aperture to generate a narrow beam on one segment. A CCD camera on the neighboring segment measures the X and Y position of the beam. Figure 4 shows a drawing of pair of sensors mounted in parallel in a single package along with the configuration of four IDSs along the edge between two segments. This configuration has eight output values and measures the 6DoF perturbations between the two segments.

The IDS exploits the high precision of the photolithography used to fabricate inexpensive CCDs and the stability of carefully mounted components. It offers the advantage of making measurements across large gaps without the necessity of physical contact or carefully controlled positioning. The measurement range is limited by the size of

the CCD to ~ 4 mm but the allowed displacement for the two ends of the IDS without damage is essentially unlimited, making installation and manipulation easy.

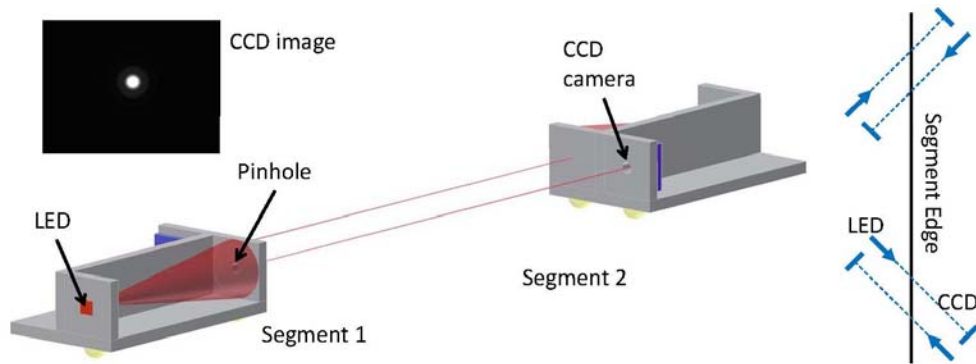


Fig. 4. Sensor configuration. The drawing on the left shows a pair of IDSs in the same package along with a CCD image from the prototype IDS. A configuration of four IDSs along the boundary between two segments that measures the 6DoF is shown on the right.

A prototype IDS has been built with the LED located 100 mm from a 100 μm pinhole and the CCD 100 mm from the pinhole. The monochrome CCD camera has 640x480 7.4 μm square pixels and outputs raw tif format images. The spot diameter on the CCD is ~ 300 μm and is fully saturated in the center for a 1/30th sec exposure. A centroiding algorithm has been developed which solves for the spot position with an accuracy of better than 1/200th of a pixel in a single frame. The Allan deviation decreased from 40 nm for a single 33 msec exposure to <1 nm for a 100 sec average of images taken at 30 frames/sec and remained below 100 nm for the four month duration of the tests. The measured dependence on LED brightness is negligible and the measured temperature dependence of the centroid position is ~ 10 nm/C. The temperature dependence appears to be dominated by the Aluminum housing used for the prototype.

4. Summary and Conclusion

CCAT presents several design challenges, especially achieving the 10 μm rms HWFE and 0.2" pointing precision. These challenges have been addressed by developing a novel CFRP truss and tipping structure supporting compound segments consisting of small reflector tiles mounted on CFRP subframes. A sophisticated surface control system based on estimating the wavefront state from the IDSs mounted on the segments has been developed and evaluated using the gravity and thermal distortions calculated from an FEA of the telescope structure. A prototype IDS demonstrates that the 6DoF relative motion between neighboring segments can be measured with a precision better than 0.1 μm and 1 μrad . A full system analysis including FEA of the major telescope components, control system and demonstrated IDS performance show that this design concept will meet the demanding CCAT requirements.

6. Acknowledgments

This work was supported by the John B. and Nelly Kilroy Foundation and by the Jet Propulsion Laboratory, California Institute of Technology, under contract with the National Aeronautics and Space Administration.

7. References

1. S. Padin, et al., "CCAT Optics," *Proc. SPIE*, 2010. **7733**: pp. 4Y-1-11.
2. D. P. Woody, S. Padin and T. A. Sebring, "CFRP truss for the CCAT 25m diameter submillimeter-wave telescope " *Proc. SPIE*, 2010. **7733**: pp. 2B-1-10.
3. D. P. Woody, et al., "Panel options for large precision radio telescopes," *Proc. SPIE*, 2008. **7018**: pp. OT1-OT11.
4. T. S. Mast and J. E. Nelson, *The Figure Control of Segmented Telescope Mirrors*, in *Keck Observatory Reports*. 1983, Keck Observatory.
5. D. C. Redding, et al., "Wavefront controls for a large submillimeter-wave observatory " *Proc. SPIE*, 2010. **7733**: pp. 29-1-11.
6. J. Z. Lou, et al., "Modeling a large submillimeter-wave observatory " *Proc. SPIE*, 2010. **7733**: pp. 26-1-13.